Anchor University Journal of Science and Technology (AUJST)
A publication of the Faculty of Science and Science Education, Anchor University Lagos

URL: journal.aul.edu.ng

In AJOL: https://www.ajol.info/index.php/aujst

Vol. 2 No 2, December 2022, Pp. 37 - 47

ISSN: 2736-0059 (Print); 2736-0067 (Online)

Investigation of groundwater potential in Atan-Ota, Ogun State, South-western Nigeria

***Joel E.S., Oyanameh O.E, Fatoye O.V., Ayeni J.K, Sunday,R.M.**

Department of Earth Sciences, Anchor University Lagos

Corresponding Author:
ejoel@aul.edu.ng

Competing Interests: The authors declare no competing interests.

ABSTRACT

Background: Potable water is one of the major resources that a citizen of any nation can benefit from and this is so because water is a free course of nature.
Objectives: Investigation of groundwater potential in Atan-Ota has been carried out with the objective of determining the depth to aquifer in the study area.
Methods: Geo-electrical resistivity technique using both 2D and Vertical Electrical Sounding (1D) method were applied with the use of PAS earth resistivity meter. Six (6) profiles were used in carrying out the investigation using both Wenner and Schlumberger array configuration. The data was interpreted using RES2DINV for 2D and computer iteration method (WinResist) for VES.
Results: The findings showed that five (5) layer- lithologies namely topsoil, lateritic clay, clayey-sand, sand (main aquifer) and shale were delineated for VES 1 and VES 2 while four (4) lithologies namely topsoil, lateritic clay, clayey-sand, sand (main aquifer) were delinaeted for VES 3 and VES 4 respectively. The apparent resistivity for the VES 1 ranged from 360.0 Ωm to 1216.2 Ωm with corresponding thickness and depth ranged between 3.4 m and 50.2 m, and 3.5 m and 111.5 m respectively. VES 2 has characteristic type of KHA with the resistivity relationship of $\rho1< \rho2> \rho3< \rho4< \rho5$ and the resistivity, thickness and depth of the lithological layers ranged from 42.5 Ω m to 710.5 Ωm, 1.4 m to 23.2 m and 1.4 m to 48.0 m respectively. The VES 3 has resistivity, thickness and depth values ranged between 48.2 Ωm and 1825.4 Ωm, 1.2 m and 31.0 m, and 1.2 m and 70.8 m respectively. Also, the VES 4 the resistivity relationship of $\rho1< \rho2> \rho3< \rho4$ which of KH curve type. The resistivity values, thickness and depth ranged from 318.4 Ωm to 7634.6 Ωm, 1.7 m to 34.1 m and 1.7 m to 41.4 m respectiveley.
Conclusions: The investigation revealed that the depth to the water-table in the study area ranged between aquifer ranges between 40 m and 111 m.

Keywords: Potable-water, groundwater, geoelectrical-resistivity, depth, aquifer

INTRODUCTION

Potable water is one of the major resources that a citizen of any nation can benefit from (Alile and Amadasun, 2008) and this is so because water is a free course of nature. The term "groundwater" is used for water which occurs beneath the ground surface. It is an important constituent of hydrological cycle and plays a major role in augmenting water supply to meet the major increasing demands in various sectors (Biswas et al., 2012; McLachlan et al., 2017; Joel et al.,2019). These sectors include manufacturing industry, agricultural industry, transportation industry, construction industry, home usage and so on (Joel et al.,2019). Groundwater occurs in the upper layers of the earth's crust and these layers consist of igneous, sedimentary and metamorphic rocks. During their origin and later evolution, these rocks develop porous and permeable structures containing pore spaces. As a result of probing these layers in assessing groundwater-resources, new technology has been developed for its searching known as geophysical technology. There are parameters that characterized groundwater and requires the use of geophysical technology in probing it; such parameters include conductivity, porosity, permeability and transmissivity (Joel et al., 2019).

Geo-electrical resistivity survey is among the geophysical technology often used to search for groundwater in both porous and fissured media. This method has been developed greatly and has become an important instrument in hydrological studies, hydrogeological prospecting etc. (Griffiths et al; 1990; Griffiths and Barker, 1993; Dahlin and Loke; Aizebeokhai et al; 2010; Alile and Amadasun, 2008; Badmus and Olatinsu, 2010; Chen et al., 2018; Dastanboo et al., 2020; Alarifi et al., 2022; Alzahrani et al., 2022). The underlying principle that describe the measurement of subsurface variation with the use geo-electrical resistivity beneath the earth was propounded by Schlumberger who performed the earliest experiment in the year 1912. In addition, the same idea was also developed by Frank Wenner in the year 1966 (Kunetz, 1966). However, geo-electrical resistivity surveys have undergone significant changes in over twenty years ago. Furthermore, the orthodox way of horizontal layering technique in the investigation of subsurface using geo-electrical resistivity data are rapidly being replaced with 2-D and 3-D models of interpretation particularly in complex and heterogeneous subsurface media. The field techniques have undergone advancement from the manual measurements being conducted at separate and independent points to the use of automated machine where multi-electrode array along the measurement profile are used. As a result, fast automated multi-electrode and multichannel data acquisition system now in existence that follows flexibility in acquiring geo-electrical resistivity data (Barker, 1981; Stummer and Maurer, 2001; Auken et al; 2006; Magnusson, 2008; Ogilvy et al., 2009; Moller et al., 2011). Therefore, due to successful application of geo-electrical resistivity over the years in search of groundwater location, this propels the use of geo-electrical resistivity method for this investigation. First of all, to delineate geological structure controlling occurrence of groundwater in the study area. Secondly, to investigate the potentiality of groundwater in the area of study. Lastly, to determine the actual depth to aquifer that stored the groundwater in large quantity.

2. Geological and hydrogeology description of the study area

The study area falls within the eastern Dahomey Basin (Figure 1). The sediments represented within the basin have a total thickness of about 3000m and include sandstone, arkoses, shale, shelly shallow water limestone, unconsolidated sands and soft marine clays. The subsurface geology comprises, from top to bottom, Alluvial sediments, Coastal Plain Sands, Ilaro Formation, Ewekoro Formation, and Abeokuta Group, overlying the Basement Complex. The Alluvial deposits consist of loose sands, silt and clay mixed in varying proportions. The clays are brownish to whitish in colour. The sorting is usually poor. The Coastal Plain Sands consists of soft, very poorly sorted, clayey sands, pebbly sands and sandy clays. The Ilaro Formation comprises coarse, angular and poorly sorted sands with a considerable clay fraction. The Ewekoro Formation in the type area consists of a limestone member about 30m thick overlain by a shale member nearly 120 m in thickness. At the outcrop, the top of the formation is marked by the appearance of sands, which occur at the base of the Ilaro Formation. The lower part of the Abeokuta Group consists of a thick argillaceous member overlying the basal sands while in the upper part sands form a much smaller proportion. Hydro-geologically, the sand units within the basin are good aquifers system.

3. Basic Theory and Field Procedure

3.1. Basic Theory

All resistivity methods employ an artificial source of current which is introduced into the ground through point electrodes or long line contacts. The procedure is to measure potentials at other electrodes in the neighbourhood of the current flow. Electrical methods of geophysical investigations are based on the resistivity or its inverse (i.e.) conductivity of materials. The electrical resistance, R of a material is related to its physical dimension, cross sectional area, A, length, L, through the resistivity ρ or its inverse, conductivity, σ is given by (1)

$$\rho = 1/\sigma = RA/L \tag{1}$$

Low frequency alternating current is employed as source signals in the DC resistivity surveys in determining subsurface resistivity distribution. Usually a complete

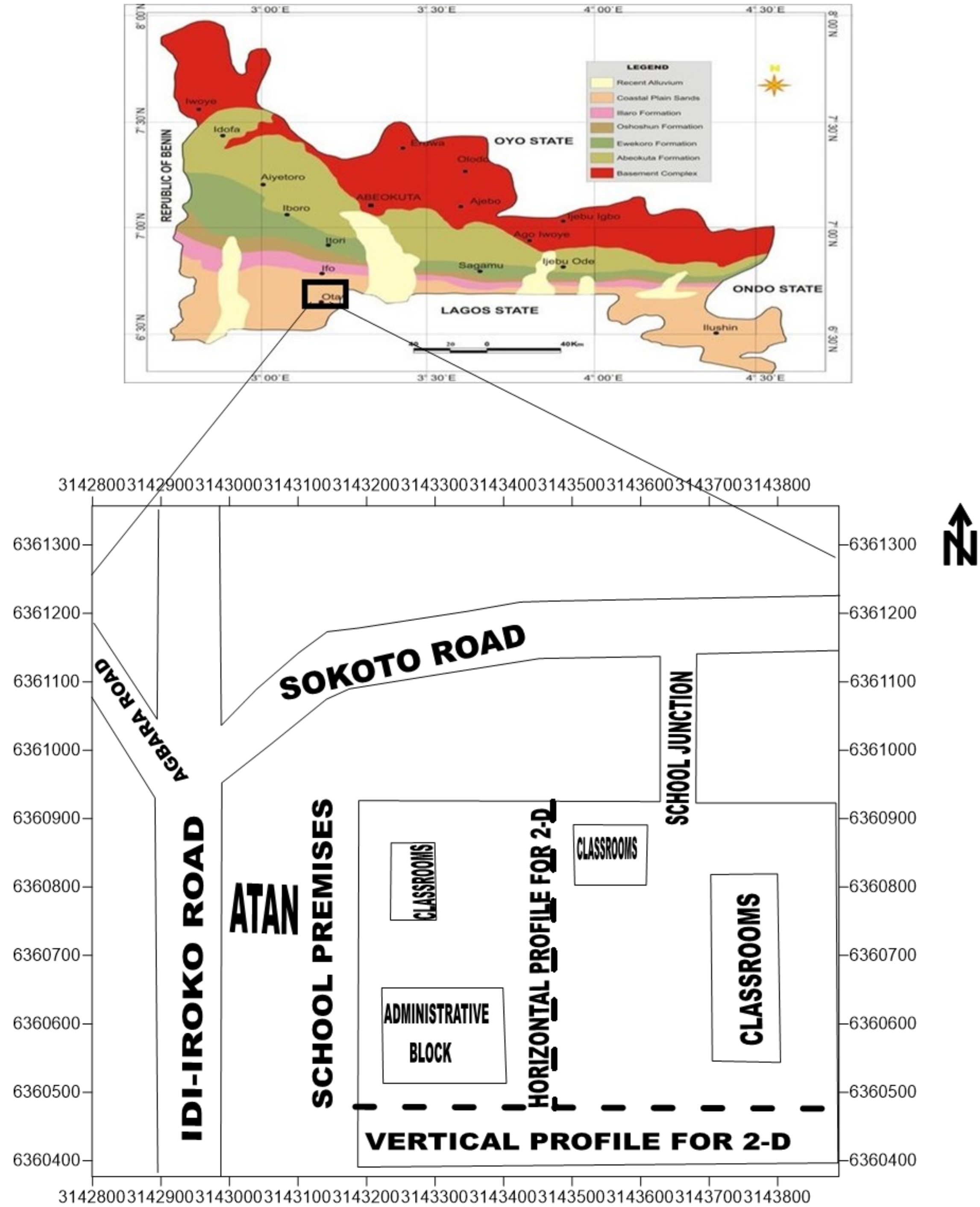

Figure 1. Geological Map of Ogun State showing the study area connected base map of the study area (Joel et al., 2016)

homogeneous and isotropic is considered. For homogeneous medium, the current density J and electric field E are related through Ohm's law (2).

$$J = \sigma E \quad (2)$$

Where E is in volts per meter and σ is the conductivity of the medium in Siemens per meter (m).

The electric field E can be represented as gradient of a scalar potential

$$E = \nabla V \quad (3)$$

$$J = \sigma \nabla V \quad (4)$$

But $\nabla . J = 0, \quad \nabla . (\sigma \nabla V) = 0$

By combining equations (2) and (3), we obtained fundamental Laplace's equation for electrostatic fields which is given by (5)

$$V^2V = 0 \qquad (5)$$

3.2. The Field Work Procedure

3.2.1. Vertical Electrical Sounding (VES)

In this investigation, both Vertical Electrical Sounding (VES) and 2-Dimensional geo-electrical resistivity surveys using Schlumberger and Wenner arrays configuration respectively were adopted in this investigation. The basic field equipment used for the study is PAS earth-resistivity meter which display apparent resistivity value digitally as computed from Ohm's law. The earth-resistivity meter is powered by 12V D.C power source. Other materials that accompany the equipment are measuring tape, 4 hammers, 45 metal electrodes where 4 metal electrodes were used for VES, cables for current and potential electrodes. In the VES where Schlumberger configuration was adopted, the four electrodes are positioned symmetrically along a straight line, the current electrodes on the outside and the potential electrodes on the inside (Figure 2). To change the depth, range of the measurements, the current electrodes are displaced outwards while the potential electrodes in general, are left at the same position. When the ratio of the distance between the current electrodes to that between the potential electrodes becomes too large, the potential electrodes must also be displaced outwards otherwise the potential difference becomes too small to be measured with sufficient accuracy (Koefoed, 1979; Alile, 2008). Measurements of current and potential electrode positions are marked such that AB/2 ≥ MN/2 (Figure 2).

Where

AB/2 = Current electrode spacing and

MN/2 = Potential electrode spacing

Generally, the arrangement consists of a pair of current electrodes and a pair of potential electrodes. These are driven into the earth in a straight line to make a good contact with the earth. The current electrode spacing is expanded over a range of values for measurements in the field. The values of AB/2 increases as the measurements progresses while the potential electrodes separations are guided accordingly. The potential electrodes are kept at small separations relative to the current electrodes separations (Milson, 1939; Alile, 2008). One of the major advantages this method has over other methods is that only the current electrodes need to be shifted to new position for most readings while potential electrodes are kept constant for up to three or four readings (Alile, 2008). During the field work taking a sounding, the PAS earth resistivity meter performs automatic recording of both voltage and current, stacks the results, computes the resistance in real time and digitally displays it. Alile, 2008). For the interpretation of Vertical Electrical Sounding, software called WinResist was used which generate or show the wavelike pattern of apparent resistivity and electrode spacing accordingly (Sharma, 1999).

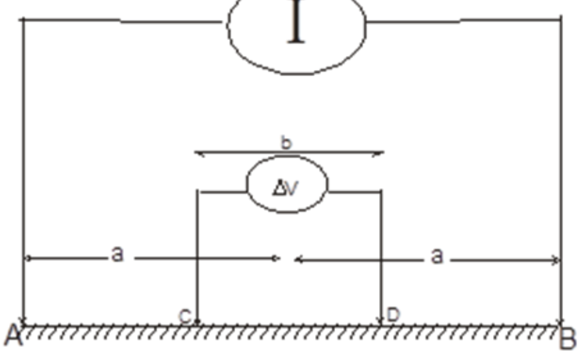

Figure 2: Schlumberger array configuration

$$V_c = \frac{\rho I}{2\pi}\left\{\frac{1}{a-b/2} - \frac{1}{a+b/2}\right\} \quad (6)$$

Where

$a \Rightarrow$ midpoint $\Rightarrow$ distance between the current electrodes and station.

b $\Rightarrow$ distance between potential electrodes

$\rho \Rightarrow$ layer resistivity

The potential at D due to A becomes

$$V_D = \frac{\rho I}{2\pi}\left\{\frac{1}{a+b/2} - \frac{1}{a-b/2}\right\} \quad (7)$$

The potential difference dV between the two potentials is therefore given by

$$dV = V_C - V_D \quad (8)$$

$$\therefore dV = \frac{\rho I}{2\pi}\left\{\frac{1}{a-b/2} - \frac{1}{a+b/2}\right\} - \left[\frac{\rho I}{2\pi}\left\{\frac{1}{a+b/2} - \frac{1}{a-b/2}\right\}\right] \quad (9)$$

$$dV = \frac{\rho I}{2\pi}\left\{\frac{2}{a-b/2} - \frac{2}{a+b/2}\right\} \quad (10)$$

$$dV = \frac{\rho I}{2\pi}\left(\frac{8b}{4a^2 - b^2}\right) \quad (11)$$

The apparent resistivity value is the product of the geometric factor and the resistance recorded in the resistivity meter. In each station, several soundings and apparent resistivity values will be obtained by expanding the current electrode spacing after each reading as required by Schlumberger array for deeper penetration into the earth and structural responses. The geometric factor, K, for Schlumberger configuration will be used. That is

$$K = \frac{\pi}{2}\left\{\frac{(AB/2)^2 - (MN/2)^2}{MN/2}\right\}$$

$$K = \pi CD\left\{\left(\frac{L}{CD}\right)^2 - 0.25\right\}$$

$$\therefore L = 2(AB/2) \quad (12)$$

$$\rho_a = KR = KV/I = \{(\pi CDV)/(I)\}\{(L/CD)^2 - 0.25\} \quad (13)$$

Where

ρ_a = apparent resistivity

R = resistance recorded in the resistivity meter

K = geometric factor

I = current

3.2.2. 2-Dimensional Resistivity Techiques Procedure

In this investigation, 2-Dimensional geo-electrical resistivity data was collected using the programmable PAS earth resistivity meter. This earth resistivity meter has a multicore cable to which electrodes were connected at take outs moulded on at predetermined equal intervals. A computer-controlled system was then used to select the active electrodes for each electrode set-up automatically. This computer-controlled system was included in the PAS earth resistivity meter which was used in the survey. The Wenner arrays were used on the two profiles line which has maximum length spread of 220m and minimum electrode spacing of 5.0 m. The data were generated along this profiles. The first profile was vertically positioned with length spread of 220m and second profile was horizontally positioned with the same maximum length spread used in the first profile. Four (4) vertical Electrical Sounding were carried out in other to determine the depth of groundwater of the study area. This is done with the use of PAS earth resistivity meter using Schlumberger array configuration. The data was processed or interpreted to generate 2D resistivity earth models using RES2DINV software developed by Loke and Barker (1996). This program uses a forward modeling subroutine to calculate apparent resistivity values from field data which are then inverted using a non-linear Least-squares optimization technique (Loke and Barker, 1996). The inversion routine in RES2DINV is based on the smoothness-constrained least-squares method (Sasaki 1992; Joseph et. al., 2006) but there is an option to use the quasi-Newton or the Gauss-Newton optimization techniques to implement the least-squares method. Both techniques at different iteration stages were combined to generate 2D resistivity models. The iterative process proceeds as follows:

(1) the inversion routine produces an initial model of subsurface resistivity using the calculated apparent resistivity values and generates a response resistivity field based on the initial model.

(2) it calculates a root mean square (RMS) value that describes the level of agreement between the synthetic and observed resistivity fields.

A large RMS value usually > 5 % indicates a poor fit. In this case, the initial model is adjusted iteratively until the RMS falls below the preset or desired threshold after which the iterative process is terminated. Due to the differential level of noise in the data, it was necessary to manipulate the damping factor in some cases to achieve stability in the inversion process. The damping factor is a parameter whose value depends on the level of random noise present in the data (Sasaki, 1992). A higher damping factor is needed for data with a high level of random noise and vice versa.

4. Results and Discussions

4.1. Vertical Electrical Sounding (VES) Result

Figures 3 to 6 present the processed VES 1 to VES 4 measured data that was directly measured from the field. Five (5) layer- lithologies namely topsoil, lateritic clay, clayey-sand, sand (main aquifer) and shale were delineated for VES 1 and VES 2 while four (4) lithologies namely topsoil, lateritic clay, clayey-sand, sand (main aquifer) were delinaeted for VES 3 and VES 4 respectively. The lithology-layers contributes to the development of groundwater because it is the passage for the flow of surface water to the fractured layers. The topsoil generally consists of three parts: the belt of soil water at the top, the intermediate vadose zone and the capillary fringe at the bottom.The delineation of the resistivity values for the lithologies layers are shown in Table 1. The first lithology layer (named topsoil) resistivity values ranged from 42.5 Ωm to 1216.1 Ω m.

The resistivity of the second layer (lateritic clay) as shown in Table 1 ranged between 409.8 Ωm and 445.0 Ωm for VES 1 , VES 2 and VES 3 while the thickness varies between 5.6 m and 38.6 m except for the VES 4 which has the highest apparent resistivity value of 7634.6 Ωm with the thickness of 5.6 m. In addition, the third layer has resistivity values of 79.9 Ωm, 360.0 Ωm and 318.4 Ωm for VES 2, VES 1 and VES 4 respectively except for VES 3 which has the highest resistivity value of 1269.9 Ωm.

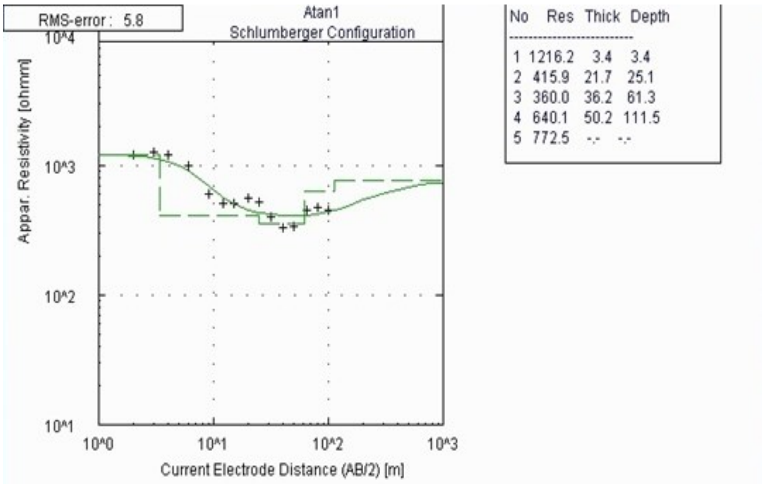

Figure 3: Showing typical curve for

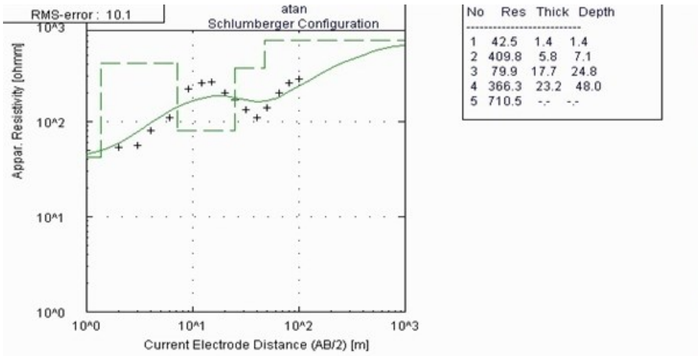

Figure 4: Showing typical curve for VES 2

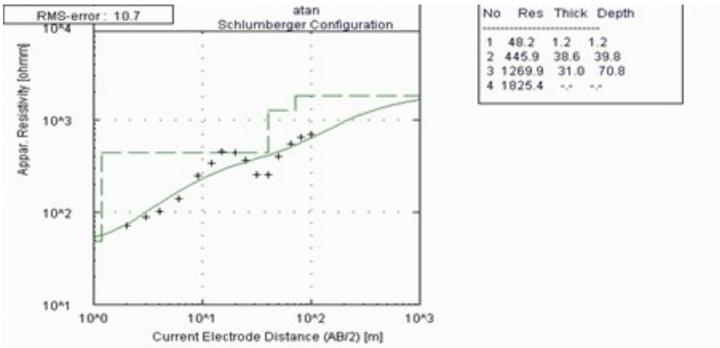

Figure 5: Showing typical curve for VES 3

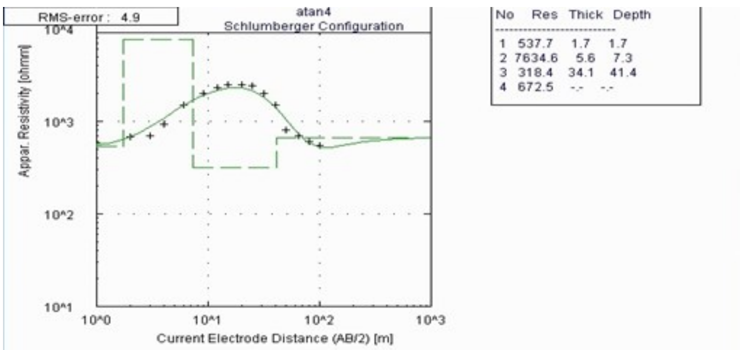

Figure 6. Showing typical curve for VES 4

The variations in the thickness ranged from 17.7 m to 36.2 m. The fourth lithology layer is sand (main aquifer) has resistivity values ranging from 640.1 Ωm to 1825.4 Ωm.

The detail description for VES 1 is shown in Table 1. The apparent resistivity for the VES 1 ranged from 360.0 Ωm to 1216.2 Ωm and it has five (5) lithological layers namely topsoil, lacteric clay, clayey-sand, sand and shale. The thickness and depth of the lithological layers ranged between 3.4 m and 50.2 m, and 3.5 m and 111.5 m respectively. The curve type characteristics is QHA types with resistivity relationship of $\rho1 > \rho2 > \rho3 < \rho4 < \rho5$. In observing VES 1, it was noticed that the depth of groundwater around the study area may be at the depth 111.5 m. Furthermore, VES 2 has characteristic type of KHA with the resistivity relationship of $\rho1 < \rho2 > \rho3 < \rho4 < \rho5$ and the lithology comprise of five (5) layers which include topsoil, lacteric clay, clayey-sand, sand and shale. The resistivity, thickness and depth of the lithological layers ranged from 42.5 Ωm to 710.5 Ωm, 1.4 m to 23.2 m and 1.4 m to 48.0 m respectively. The VES 3 has resistivity, thickness and depth values ranged between 48.2 Ωm and 1825.4 Ωm, 1.2 m and 31.0 m, and 1.2 m and 70.8 m respectively. The lithology of VES 3 comprise of four (4) layers namely topsoil, lacteric clay, clayey-sand and sand, resistivity relationship of $\rho1 < \rho2 < \rho3 < \rho4$ and curve type of AA. Also, the VES 4 has four (4) lithological layers which are topsoil, lacteric clay, clayey-sand and sand, the resistivity relationship of $\rho1 < \rho2 > \rho3 < \rho4$ which of KH curve type. The resistivity values, thickness and depth ranged from 318.4 Ωm to 7634.6 Ωm, 1.7 m to 34.1 m and 1.7 m to 41.4 m respectiveley. Generally, it was obserevd that there three (3) level of aquifers that can be tapped from the study area which are high -yield aquifer at depth of 111.5 m, moderate-yield aquifer at depth of 70.8 m and low-yield aquifer at the depth of 41.4 m and 48.2 m.

Table 1. The detail description of apparent resistivity curve

VES Number	Layer Resistivity in Ωm	No of layers	Thickness (m)	Depth (m)	Resistivity Relationship	Type Curve	Inferred lithology
1							
	1216.2 415.9 360.0 640.1 772.5	5	3.4 21.7 36.2 50.2 ----	3.5 25.1 61.3 111.5 ----	$\rho1 > \rho2 > \rho3 < \rho4 < \rho5$	QHA	Topsoil Lateritic- Clay Clayey-sand Sand Shale
2							
	42.5 409.8 79.9 366.3 710.5	5	1.4 5.8 17.7 23.2 ----	1.4 7.1 24.8 48.0 ----	$\rho1 < \rho2 > \rho3 < \rho4 < \rho5$	KHA	Topsoil Lateritic- Clay Clayey sand Sand Shale
3							
	48.2 445.9 1269.9 1825.4	4	1.2 38.6 31.0 ----	1.2 39.8 70.8 ----	$\rho1 < \rho2 < \rho3 < \rho4$	AA	Topsoil Lateritic- Clay Clayey sand Sand
4							
	537.7 7634.6 318.4 672.5	4	1.7 5.6 34.1 ----	1.7 7.3 41.4 ----	$\rho1 < \rho2 > \rho3 < \rho4$	KH	Topsoil Lateritic- Clay Clayey sand Sand

4.2. 2-Dimensonal Resistivity Processed Result

The geological map of Ogun State shows that Atan is mainly dominated by coastal plain sands. From the inverse model section, the first layer in the structure has the highest resistivity value that ranges between 30,255 Ω.m to 85,319 Ω.m. This value of resistivity indicates that the first layer is lateritic-clay which has such high resistivity and naturally reflects the geological nature of the study area. The second layer with resistivity value of 3800 Ω.m to 10,757 Ω.m represents coarse sand. The resistivity value between 950 Ω.m and 1356 Ω.m indicates that the third layer is mudstone which is consolidated in nature. The resistivity's value ranges between 300Ω.m to 940 Ω.m which is fourth layer in the structure represent mud-clay which is sandy in nature. The resistivity ranges between 60.7 Ω.m and approximately 280 Ω.m which is an indication of presence of fresh groundwater (Figure 7). However, the aquifer resistivity value of a place varies and this depends on the nature of the subsurface of the study area.

The profile 2 of this survey was positioned horizontally and perpendicularly to the first profile. Figure 8 showed the inverse model resistivity section for profile 2. From the result it indicates that lateritic-clay which is first layer is having approximate resistivity value that ranges between 1200 Ω.m to 3000 Ω.m. The second layer of this second profile has resistivity value ranges between 800 Ω.m to 1000 Ω.m which indicates coarse sand. The resistivity value that ranges between 500 Ω.m to 800 Ω.m approximately represents mudstone which is third layer. The resistivity value between 200 Ω.m and 400 Ω.m represent the presence of groundwater which can contain mud.

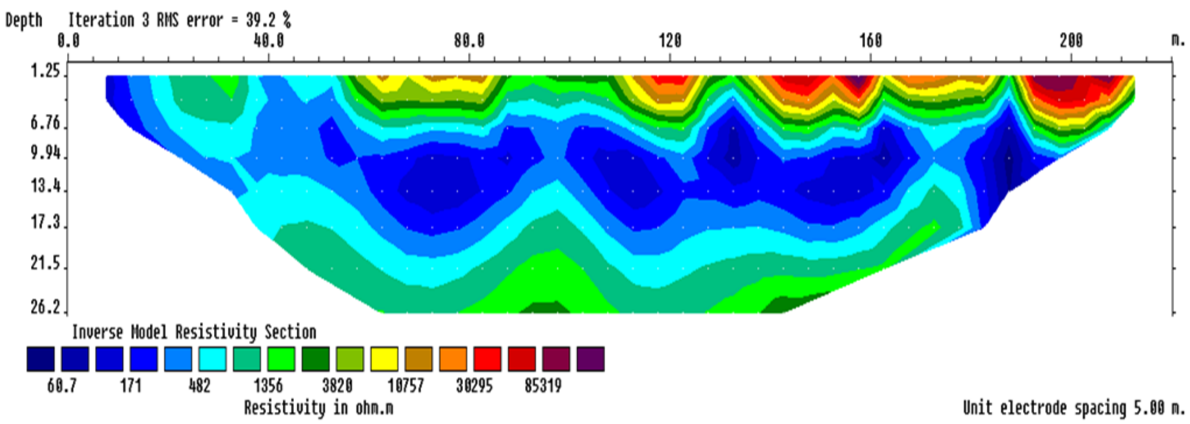

Figure 7. Inverse model resistivity section for profile 1

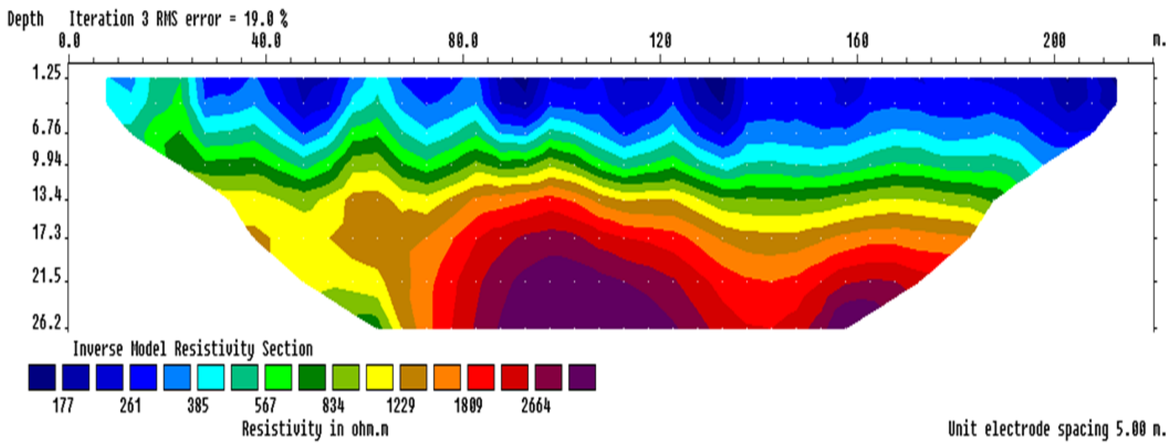

Figure 8. Inverse model resistivity section for profile 1

5. Conclusions

Investigation of groundwater potential in Atan-Ota South-western Nigeria has been carried out with the use of combination of Vertical Electrical Sounding (VES) and 2D resistivity techniques. The results from the VES showed that the subsurface of the study area has varied lithology. Five (5) layer- lithologies namely topsoil, lateritic clay, clayey-sand, sand (main aquifer) and shale were delineated for VES 1 and VES 2 while four (4) lithologies namely topsoil, lateritic clay, clayey-sand, sand (main aquifer) were delinaeted for VES 3 and VES 4 respectively. The apparent resistivity for the VES 1 ranged from 360.0 Ωm to 1216.2 Ωm with corresponding thickness and depth ranged between 3.4 m and 50.2 m, and 3.5 m and 111.5 m respectively. VES 2 has characteristic type of KHA with the resistivity relationship of $\rho1 < \rho2 > \rho3 < \rho4 < \rho5$ and the resistivity, thickness and depth of the lithological layers ranged from 42.5 Ωm to 710.5 Ωm, 1.4 m to 23.2 m and 1.4 m to 48.0 m respectively. The VES 3 has resistivity, thickness and depth values ranged between 48.2 Ωm and 1825.4 Ωm, 1.2 m and 31.0 m, and 1.2 m and 70.8 m respectively. Also, the VES 4 has four (4) lithological layers which are topsoil, lacteric clay, clayey-sand and sand, the resistivity relationship of $\rho1 < \rho2 > \rho3 < \rho4$ which of KH curve type. The resistivity values, thickness and depth ranged from 318.4 Ωm to 7634.6 Ωm, 1.7 m to 34.1 m and 1.7 m to 41.4 m respectiveley. Generally, it was obserevd that there three (3) level of aquifers where groundwater can be tapped exist within the study area which are high-yield aquifer at depth of 111.5 m, moderate-yield aquifer at depth of 70.8 m and low-yield aquifer at the depth of 41.4 m and 48.2 m and the borehole siting should be done in East–West direction.

Acknowlegdements
The authors appreciate the management of Anchor University Lagos for providing the enabling environment in carrying out this research

References

Alarifi, S.S. Abdelrahman, K., Hazaea, B. Y. (2022). Depicting of groundwater potential in hard rocks of southwestern Saudi Arabia using the vertical electrical sounding approach, Journal of King Saud University - Science, 34, (7), 102221. Doi.org/10.1016/j.jksus.2022.102221.

Alile, Owns. M. And Amadasun, C.V.O. (2008): Direct Current Probing of the Subsurface Earth for Water Layer in Oredo Local Government Area, Edo State, Nigeria. Nigeria Journal of Applied Science, Vol. 25: 107 – 116.

Alzahrani, H., Abdelrahman, K., Saddam, S.A (2022). Use of geoelectrical resistivity method for detecting near-surface groundwater potential zones at Riyadh city, Saudi Arabia, Journal of King Saud University -Sciences, 34, (7), 102253, https://doi.org/10.1016/j.jksus.2022.102253.

Aizebeokhai A.P, Olayinka A.I, Singh V.S (2010): Application of 2D and 3D Geo-electrical Resistivity Imaging for Engineering Site Investigation in a Crystalline Basement Terrain,

Auken. E, Pellerin. L, Christensen N.B, Sorenson. K (2006): A survey of current trends in near surface electrical and electromagnetic methods. Geophys, 71 (5): 249-260.

Biswas, A., Jana, A., Sharma, S.P., 2012. Delineation of groundwater potential zones using satellite remote sensing and geographic information system techniques. A case study from Ganjam district, Orissa, India. Research Journal of Recent sci 1 (9), 59–66.

Badmus and Olatinsu (2010): Aquifer Characteristics and Groundwater Recharge Pattern in Typical Basement Complex: A case study of Federal College of Education, Osiele, Abeokuta, Southwestern, Nigeria. African Journal Environmental Science Technology. 328-342.

Barker R.D (1981): The Offset System of Electrical Resistivity Sounding and Its Use with Multicore Cable. Geophy. Prosp. 29: 128-143.

Chen, W., Li, H., Hou, E., Wang, S., Wang, G., Panahi, M., Ahmad, B.B. (2018). GIS – based groundwater potential analysis using novel ensemble weights of evidence with logistic regression and functional tree models. Science of the Total Environment, 634, 853-867. Doi: 10.1016/j.scitotenv.2018.04.055.

Dahlin. T and Loke M.H (1998): Resolution of 2D Wenner Resistivity Imaging as Assessed by Numerical Modeling. J. Apply. Geophys. 29:211 – 226.

Dastanboo, Nima, Li, Xiao-Qing and Gharibdoost, Hamed. “Comparison between electrical resistivity tomography and tunnel seismic prediction 303 methods for detecting the water zone ahead of the tunnel face: A case study” *open Geosciences,* vol. 12, no. 1, 2020, pp. 1094 – 1104. Https://doi.org/10.1515/geo-2020-0193.

Griffiths D.H, Barker R.D (1993): Two-dimensional resistivity imaging and modeling in Areas of Complex Geology. J. Appl. Geophys., 29:211-216.

Griffths D.H, Turnbull J, Olayinka A.I (1990): Two-dimensional Resistivity Mapping with a Complex Controlled Array. First Break, 8:121-129.

Joel, E. S., Olasehinde, P.I., Adagunodo, T.A., Omeje, M., Akinyemi, M.L., Ojo, J.S. (2019): Integration of aeromagnetic and electrical resistivity imaging for groundwater potential assessments of coastal plain sands area of Ado-Odo/Ota in southwest Nigeria. Groundw. Sustain. Dev. 9 (2019), 100264 (2019).

Joseph T. Zume, Aondover Tarhule and Scott Christenson (2006): Subsurface Imaging of an Abandoned Solid Waste Landfill Site in Norman Oklahoma. National Groundwater Association. Pp 62-69.

Kunetz.G. (1996): Principles of Direct Current Resistivity Prospecting. Gebruder Borntraeger, Berlin, p. 103.

Loke M.H and Barker R.D, (1996): Practical Techniques for 3D Resistivity Surveys and Data Inversion. Geophys. Prosp, 44: 499-524.

Mclachlan, P.J. Chambers, J.E. Uhlemann, Binley, S.S., 2017. A. Geophysical characterisation of the groundwater-surface water interface. Adv. Water Resour. 109, 302–319.

Mimm K. Magnusson, (2008). Geoelectrical Imaging for Interpretation of Geological Conditions Affecting Quarry Operations KTH Architecture and the Built Environment. TRITA-LWR. LIC 2044.

Moller Ingelise, Jacobian Bo.H and

Christenson, Niels. B (2011): Rapid Inversion of 2D Geoelectrical Data by Multichannel Deconvolution. Society of Exploration Geophysicists.

Ogilvy R.D, Kuras O. Meldrum P.I, Palumbo- ROE. B, Wilkinson PB, Chambers, J.E and Klinck B.A (2009). The Detection and Tracking of Mine – Water Pollution from Abandoned Mines Using Electrical Tomography. Document Transformation Technology CC.

Sasaki. Y (1982): Resolution of Resistivity Tomography Inferred from Numerical Simulation. Geophy. Prosp. 40: 453-464.

Stummer. P and Maurer H.R (2001): Real-time Experimental Design Applied to High Resolution Direct- Current Resistivity Surveys. International Symposium on Optical Science and Technology. Expanded Abstracts, 143- 150.

Sharma. V. Prem (1999): Environmental and Engineering Geophysics. Pp 237- 241.